

Numerical study of the ghost-gluon vertex in Landau gauge

To cite this article: Attilio Cucchieri *et al* JHEP12(2004)012

View the [article online](#) for updates and enhancements.

You may also like

- [Emergence of mass in the gauge sector of QCD](#)
J. Papavassiliou
- [A window on infrared QCD with small expansion parameters](#)
Marcela Peláez, Urko Reinosa, Julien Serreau et al.
- [Global solvability and stabilization to a cancer invasion model with remodelling of ECM](#)
Chunhua Jin

Numerical study of the ghost-gluon vertex in Landau gauge

Attilio Cucchieri, Tereza Mendes and Antonio Mihara

Instituto de Física de São Carlos, Universidade de São Paulo

C.P. 369, 13560-970 São Carlos, SP, Brazil

E-mail: attilio@if.sc.usp.br, mendes@if.sc.usp.br, mihara@ift.unesp.br

ABSTRACT: We present a numerical study of the ghost-gluon vertex and of the corresponding renormalization function $\tilde{Z}_1(p^2)$ in minimal Landau gauge for SU(2) lattice gauge theory. Data were obtained for three different lattice volumes ($V = 4^4, 8^4, 16^4$) and for three lattice couplings $\beta = 2.2, 2.3, 2.4$. Gribov-copy effects have been analyzed using the so-called smeared gauge fixing. We also consider two different sets of momenta (orbits) in order to check for possible effects due to the breaking of rotational symmetry. The vertex has been evaluated at the asymmetric point $(0; p, -p)$ in momentum-subtraction scheme. We find that $\tilde{Z}_1(p^2)$ is approximately constant and equal to 1, at least for momenta $p \gtrsim 1$ GeV. This constitutes a nonperturbative verification of the so-called nonrenormalization of the Landau ghost-gluon vertex. Finally, we use our data to evaluate the running coupling constant $\alpha_s(p^2)$.

KEYWORDS: Lattice Quantum Field Theory, Lattice Gauge Field Theories, Lattice QCD.

Contents

1. Introduction	1
2. The ghost-gluon vertex	3
3. Numerical simulations	5
3.1 Ghost-gluon vertex on the lattice	7
4. Results	10
5. Conclusions	12

1. Introduction

In the framework of quantum field theory, Faddeev-Popov ghosts are introduced in order to quantize non-abelian gauge theories. Although the ghosts are a mathematical artifact and are absent from the physical spectrum, one can use the ghost-gluon vertex and the ghost propagator to calculate physical observables, such as the QCD running coupling $\alpha_s(p^2)$, using the relation [1]

$$\alpha_s(p^2) = \alpha_0 \frac{Z_3(p^2) \tilde{Z}_3^2(p^2)}{\tilde{Z}_1^2(p^2)}. \quad (1.1)$$

Here $\alpha_0 = g_0^2/4\pi$ is the bare coupling constant and $Z_3(p^2)$, $\tilde{Z}_3(p^2)$ and $\tilde{Z}_1(p^2)$ are, respectively, the gluon, ghost and ghost-gluon vertex renormalization functions. In Landau gauge, the vertex renormalization function $\tilde{Z}_1(p^2)$ is finite and constant, i.e. independent of the renormalization scale p , to all orders of perturbation theory (see [2] and the nonrenormalization theorems in [3, Chapter 6]). However, a direct nonperturbative verification of this result is still lacking. This is the purpose of the present work. Let us stress that, if $\tilde{Z}_1(p^2)$ is finite and constant also at the nonperturbative level, the equation above can be simplified, yielding a nonperturbative definition of the running coupling constant that requires only the calculation of gluon and ghost propagators [4, 5]. A nonperturbative investigation of the structure of the ghost-gluon vertex is also important for studies of gluon and ghost propagators using Dyson-Schwinger equations (DSE) [6]. In fact, in these studies, one makes use of Ansätze for the behavior of the propagators and vertices in the equations, in order to obtain solvable truncation schemes. Of course, a nonperturbative input for these quantities is important for a truly nonperturbative solution of the DSE.

Let us recall that in Landau gauge the gluon and ghost propagators can be expressed (in momentum space) as

$$D_{\mu\nu}^{bc}(q, -q) = \delta^{bc} \left(\delta_{\mu\nu} - \frac{q_\mu q_\nu}{q^2} \right) D(q^2) = \delta^{bc} \left(\delta_{\mu\nu} - \frac{q_\mu q_\nu}{q^2} \right) \frac{F(q^2)}{q^2} \quad (1.2)$$

$$G^{bc}(q, -q) = -\delta^{bc} G(q^2) = -\delta^{bc} \frac{J(q^2)}{q^2}, \quad (1.3)$$

where $F(q^2)$ and $J(q^2)$ are, respectively, the gluon and ghost form factor and the color indices b and c take values $1, 2, \dots, N_c^2 - 1$ in the $SU(N_c)$ case. Then, in the momentum-subtraction scheme one has that the gluon and ghost renormalization functions are given by

$$F_R(q^2, p^2) = Z_3^{-1}(p^2) F(q^2) \quad (1.4)$$

$$J_R(q^2, p^2) = \tilde{Z}_3^{-1}(p^2) J(q^2) \quad (1.5)$$

with the renormalization conditions

$$F_R(p^2, p^2) = J_R(p^2, p^2) = 1. \quad (1.6)$$

Thus, if one can set $\tilde{Z}_1(p^2) = 1$, the running coupling (1.1) can be written as [4, 5]

$$\alpha_s(p^2) = \alpha_0 F(p^2) J^2(p^2), \quad (1.7)$$

i.e. one only needs to evaluate the gluon and ghost form factors defined above. In recent years, the infrared behavior of these form factors has been extensively studied (in Landau gauge) using different analytical approaches [4, 5], [7]–[25]. Also, numerical studies of these form factors and of the running coupling defined in equation (1.7) have been reported in [26, 27, 28, 29] for the $SU(2)$ group and in [30]–[37] for the $SU(3)$ case.

An indirect evaluation of the ghost-gluon vertex renormalization function has been recently presented in [29], confirming that $\tilde{Z}_1(p^2)$ is finite in the continuum limit. On the other hand, a direct nonperturbative verification of this result from a numerical evaluation of the ghost-gluon vertex is still missing. Let us stress that a direct evaluation of $\tilde{Z}_1(p^2)$ would allow a study of the running coupling constant [38] using equation (1.1) instead of equation (1.7). Such a study may improve the precision of the determination of $\alpha_s(p^2)$, since in that case one does not need, in principle, to use the so-called *matching rescaling* technique [29] when considering data obtained at different β values.

In this paper we study numerically the ghost-gluon vertex and the corresponding renormalization function $\tilde{Z}_1(p^2)$ for the $SU(2)$ case in the minimal Landau gauge. The definition of this renormalization function (in the continuum) is presented in section 2. Numerical simulations are explained in section 3. In particular, in section 3.1 we define the vertex renormalization function on the lattice and compare our direct determination of $\tilde{Z}_1(p^2)$ to the indirect evaluation presented in [29]. Note that, since the numerical evaluation of the ghost-gluon vertex may be affected by Gribov-copy effects (see discussion in sections 3 and 4 below), we evaluate this quantity using two different gauge-fixing methods, leading to two different sets of Gribov copies. A comparison of the results obtained in the two cases allows us to estimate the influence of Gribov copies (the so-called Gribov noise) on the considered quantity.

Results for the ghost-gluon vertex renormalization function, the gluon and ghost propagators and the running coupling constant $\alpha_s(p^2)$ are reported in section 4. Finally, in section 5 we draw our conclusions. Preliminary results have been reported in [39].

2. The ghost-gluon vertex

Following the notation in reference [6] (see also figure 1) the 3-point function for A_μ^a (gluon), η^b (ghost) and $\bar{\eta}^c$ (anti-ghost) fields — corresponding to the ghost-gluon vertex — is given by

$$V_\mu^{abc}(x, y, z) = \left\langle A_\mu^a(x) \eta^b(y) \bar{\eta}^c(z) \right\rangle. \quad (2.1)$$

Going to momentum space and using translational invariance for the 3-point function, one gets

$$V_\mu^{abc}(k; q, s) = \int d^4x d^4y d^4z e^{-i(kx+qy-sz)} V_\mu^{abc}(x, y, z) \quad (2.2)$$

$$= \int d^4z e^{-i(k+q-s)z} \int d^4x d^4y e^{-i(kx+qy)} \left\langle A_\mu^a(x) \eta^b(y) \bar{\eta}^c(0) \right\rangle \quad (2.3)$$

$$= (2\pi)^4 \delta^4(k + q - s) G_\mu^{abc}(k, q), \quad (2.4)$$

where $\delta^4(k + q - s)$ implies conservation of momentum. Then, the ghost-gluon vertex function is obtained by “amputating” the corresponding 3-point function (see figure 2)

$$\Gamma_\mu^{abc}(k, q) = \frac{G_\mu^{abc}(k, q)}{D(k^2) G(q^2) G(s^2)}, \quad (2.5)$$

where $s = k + q$ and the functions $D(k^2)$ and $G(q^2)$ have been defined in equations (1.2) and (1.3), respectively. At tree level (in the continuum) one obtains [1]

$$\Gamma_\mu^{abc}(k, q) = i g_0 f^{abc} q_\mu, \quad (2.6)$$

where g_0 is the bare coupling and f^{abc} are the structure functions of the $SU(N_c)$ Lie algebra. This implies the well-known result that the ghost-gluon vertex is proportional to the momentum q of the outgoing ghost. More generally, we can write the relation [6]

$$\Gamma_\mu^{abc}(k, q) = g_0 f^{abc} \Gamma_\mu(k, q), \quad (2.7)$$

where $\Gamma_\mu(k, q)$ is the so-called reduced vertex function. Then, multiplying the previous equation by $f^{dbc} \delta^{ad}$, summing over a, b, c, d and using the relation $\sum_{b,c} f^{dbc} f^{abc} = N_c \delta^{da}$ we get

$$\Gamma_\mu(k, q) = \frac{1}{g_0 N_c (N_c^2 - 1)} \sum_{a,b,c} f^{abc} \Gamma_\mu^{abc}(k, q). \quad (2.8)$$

Since at tree level one has $\Gamma_\mu(k, q) = i q_\mu$ we can also write

$$\Gamma_\mu(k, q) = i q_\mu \Gamma(k^2, q^2) \quad (2.9)$$

and it is the scalar function $\Gamma(k^2, q^2)$ that gets renormalized, when considering a given renormalization scheme.

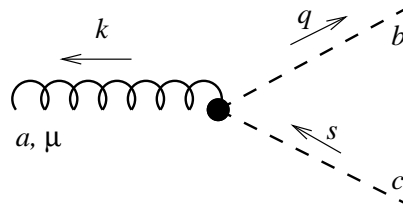


Figure 1: Notation (momenta and indices) for the ghost-gluon vertex.

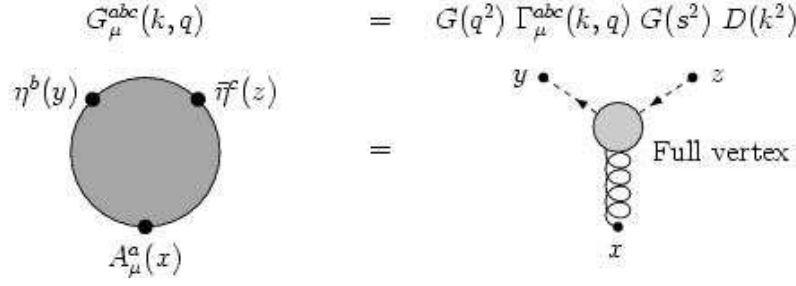


Figure 2: The 3-point function $G_\mu^{abc}(k, q)$ and its relation with the full ghost-gluon vertex $\Gamma_\mu^{abc}(k, q)$.

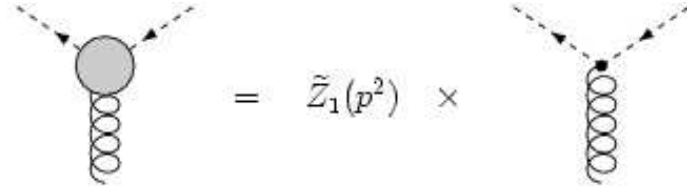


Figure 3: Relation between the full (left) and the bare (right) vertices.

Clearly, from the above relations we obtain

$$\Gamma(k^2, q^2) = \frac{-i}{q^2} \sum_\mu q_\mu \Gamma_\mu(k, q) = \frac{-i}{g_0 N_c (N_c^2 - 1)} \frac{1}{q^2} \sum_\mu q_\mu \sum_{a,b,c} f^{abc} \Gamma_\mu^{abc}(k, q). \quad (2.10)$$

In our simulations we considered the asymmetric point with zero momentum for the gluon ($k = 0$), implying $s = q$. Formula (2.10) then becomes

$$\Xi(q^2) = \Gamma(0, q^2) = \frac{-i}{g_0 N_c (N_c^2 - 1)} \frac{1}{q^2} \sum_\mu q_\mu \sum_{a,b,c} f^{abc} \Gamma_\mu^{abc}(0, q). \quad (2.11)$$

Let us note that the factor $-i$ in the equations above disappears, since only the imaginary part of the vertex function $\Gamma_\mu^{abc}(0, q)$ contributes to the quantity $\Xi(q^2)$, i.e. we can write

$$\Xi(q^2) = \frac{1}{g_0 N_c (N_c^2 - 1)} \frac{1}{q^2} \sum_\mu q_\mu \sum_{a,b,c} f^{abc} \text{Im} \Gamma_\mu^{abc}(0, q). \quad (2.12)$$

Finally, in momentum-subtraction scheme one fixes the vertex renormalization function $\tilde{Z}_1(p^2)$ by requiring (see also figure 3)

$$\Xi_R(q^2, p^2) = \tilde{Z}_1(p^2) \Xi(q^2) \quad (2.13)$$

$$\Xi_R(p^2, p^2) = 1, \quad (2.14)$$

namely the renormalized reduced vertex function $\Gamma_\mu(0, q)$ is equal to the tree-level value $i q_\mu$ at the renormalization scale. Then, the vertex renormalization function is given by

$$\tilde{Z}_1^{-1}(p^2) = \Xi(p^2). \quad (2.15)$$

We also obtain that the running coupling can be written as

$$g_s(p^2) = g_0 \tilde{Z}_1^{-1}(p^2) Z_3^{1/2}(p^2) \tilde{Z}_3(p^2) \quad (2.16)$$

$$= g_0 \Xi(p^2) F^{1/2}(p^2) J(p^2) \quad (2.17)$$

$$= \frac{1}{N_c(N_c^2 - 1)} \frac{F^{1/2}(p^2) J(p^2)}{p^2 D(0) G^2(p^2)} \sum_{\mu} p_{\mu} \sum_{a,b,c} f^{abc} \text{Im} G_{\mu}^{abc}(0, p) \quad (2.18)$$

$$= \frac{1}{N_c(N_c^2 - 1)} \frac{F^{1/2}(p^2)}{D(0) G(p^2)} \sum_{\mu} p_{\mu} \sum_{a,b,c} f^{abc} \text{Im} G_{\mu}^{abc}(0, p), \quad (2.19)$$

where we used equation (1.3).

3. Numerical simulations

For the simulations (see [40] for details) we consider the standard Wilson action, thermalized using heat-bath [41] accelerated by *hybrid overrelaxation* [42, 43, 44]. Since we are considering the SU(2) gauge group we parametrize the link variables $U_{\mu}(x)$ as

$$U_{\mu}(x) = u_{\mu}^0(x) \mathbb{1} + i \vec{u}_{\mu}(x) \cdot \vec{\sigma}, \quad (3.1)$$

where $\mathbb{1}$ is the 2×2 identity matrix, σ^b are the Pauli matrices and the relation

$$[u_{\mu}^0(x)]^2 + [\vec{u}_{\mu}(x)]^2 = 1 \quad (3.2)$$

is satisfied. We also consider the standard definition of the lattice gluon field, i.e.

$$A_{\mu}(x) = A_{\mu}^b(x) \sigma^b = \frac{U_{\mu}(x) - U_{\mu}^{\dagger}(x)}{2i}, \quad (3.3)$$

implying that the lattice gluon field component $A_{\mu}^b(x)$ is equal to $u_{\mu}^b(x)$. The connection between the lattice link variables $U_{\mu}(x)$ and the continuum gauge field $A_{\mu}(x)$ is given by

$$U_{\mu}(x) = \exp \left[i a g_0 A_{\mu}^b(x) t^b \right], \quad (3.4)$$

where $t^b = \sigma^b/2$ are the generators of the SU(2) algebra, a is the lattice spacing and g_0 is the bare coupling constant. Then, the lattice quantity $2 A_{\mu}^b(x)/(a g_0)$ approaches the continuum-gluon-field component $A_{\mu}^b(x)$ in the naive continuum limit $a \rightarrow 0$. Let us also recall that a generic lattice momentum \hat{q} has components (in lattice units)

$$\hat{q}_{\mu} = 2 \sin \left(\frac{\pi \tilde{q}_{\mu} a}{L_{\mu}} \right). \quad (3.5)$$

Here $L_{\mu} = a N_{\mu}$ is the physical size of the lattice in the μ direction, the quantity \tilde{q}_{μ} takes values $\lfloor \frac{-N_{\mu}}{2} \rfloor + 1, \dots, \lfloor \frac{N_{\mu}}{2} \rfloor$ and N_{μ} is the number of lattice points in the μ direction. If we keep the physical size L_{μ} constant and indicate with q_{μ} the momentum components in the continuum, we find that the lattice components $\hat{q}_{\mu} = a q_{\mu}$ take values in the interval $(-\pi, \pi]$ when $a \rightarrow 0$.

Lattice Volume $V = N^4$	4^4	8^4	16^4
No. of Configurations	1000	400	250

Table 1: Lattice volumes and total number of configurations considered.

In table 1 we show the lattice volumes used in the simulations and the corresponding numbers of configurations. For each volume we have considered three values of the lattice coupling, namely $\beta = 2.2, 2.3, 2.4$. The corresponding string tensions in lattice units [29] are, respectively, equal to $\sigma a^2 = 0.220(9), 0.136(2)$ and $0.071(1)$.

The minimal (lattice) Landau gauge is implemented using the stochastic overrelaxation algorithm [45, 46, 47]. We stop the gauge fixing when the average value of $(\nabla \cdot A)^2$ — see equation (6.1) in [47] for a definition — is smaller than 10^{-13} . The gluon and ghost propagators in momentum space are evaluated using the relations

$$D(0) = \frac{1}{12} \sum_{b,\mu} D_{\mu\mu}^{bb}(0) \quad (3.6)$$

$$D(\tilde{q}) = \frac{1}{9} \sum_{b,\mu} D_{\mu\mu}^{bb}(\tilde{q}) \quad (3.7)$$

$$G(\tilde{q}) = \frac{1}{3} \sum_b G^{bb}(\tilde{q}), \quad (3.8)$$

where

$$D_{\mu\nu}^{bc}(\tilde{q}) = \frac{1}{V} \sum_{x,y} \exp[i\tilde{q}(x-y)] \left\langle A_\mu^b(x) A_\nu^c(y) \right\rangle, \quad (3.9)$$

$$G^{bc}(\tilde{q}) = \left\langle (M^{-1})^{bc}(\tilde{q}) \right\rangle, \quad (3.10)$$

$$(M^{-1})^{bc}(\tilde{q}) = \frac{1}{V} \sum_{x,y} \exp[-i\tilde{q}(x-y)] (M^{-1})_{xy}^{bc}, \quad (3.11)$$

V is the lattice volume and M_{xy}^{bc} is a lattice discretization of the Faddeev-Popov operator $[(-\partial + A) \cdot \partial]$. The expression of this matrix in terms of the gauged-fixed link variables can be found in [48, equation (B.18)] for the generic $SU(N_c)$ case and in [49, equation (11)] for the $SU(2)$ case considered in the present work. Let us recall that this matrix has a trivial null eigenvalue corresponding to a constant eigenvector. Thus, one can evaluate the inverse of M_{xy}^{bc} only in the space orthogonal to constant vectors, i.e. at non-zero momentum. For the inversion we used a conjugate gradient method with even/odd preconditioning.

Finally, in order to check for possible Gribov-copy effects we have done (for each thermalized configuration) a second gauge fixing using the smearing method introduced in [50]. To this end we have applied the APE smearing process

$$U_\mu(x) \rightarrow (1 - w) U_\mu(x) + w \Sigma_\mu^\dagger(x), \quad (3.12)$$

where $\Sigma_\mu(x)$ represents the sum over the connecting staples for the link $U_\mu(x)$, followed by a reunitarization of the link matrix. We have chosen $w = 10/6$ and stopped the smearing

	V = 4 ⁴	V = 8 ⁴	V = 16 ⁴
$\beta = 2.2$	4.3 %	25.0 %	97.2 %
$\beta = 2.3$	4.4 %	16.8 %	72.8 %
$\beta = 2.4$	4.1 %	9.8 %	50.8 %

Table 2: Percentage of configurations for which the smeared gauge fixing has found a (different) Gribov copy. Results are reported for the three lattice volumes and the three β values considered.

	V = 4 ⁴	V = 8 ⁴	V = 16 ⁴
$\beta = 2.2$	46.5 %	52.0 %	63.8 %
$\beta = 2.3$	38.6 %	52.2 %	65.4 %
$\beta = 2.4$	39.0 %	48.7 %	65.4 %

Table 3: Percentage of (different) Gribov copies for which the smeared gauge fixing has found a smaller value of the minimizing function. Results are reported for the three lattice volumes and the three β values considered.

when the condition

$$\frac{Tr}{2} \overline{W}_{1,1} \geq 0.995 \quad (3.13)$$

was satisfied. (This is usually achieved with a few APE-smearing sweeps.) Here $W_{1,1}$ is the 1×1 loop and the average is taken over all $W_{1,1}$ loops of a given configuration. The gauge fixing for the smeared configuration as well as the final gauge-fixing step have been done again using the stochastic overrelaxation algorithm. The smeared gauge-fixing method is supposed to find a unique Gribov copy, even though this copy does not always correspond to the absolute minimum of the minimizing functional [50]. In our simulations we found that the number of *different* Gribov copies obtained with the smeared gauge fixing increases with larger lattice volumes and with smaller β values (see table 2). This is in agreement with previous studies [51, 52, 53] and it should be related to an increasing number of local minima for the minimizing function when the system is highly disordered. We also found that the minimum obtained with the smeared gauge fixing is not always smaller than the one obtained without smearing, but at larger lattice volumes the smearing approach seems to be more effective in getting closer to the absolute minimum of the minimizing function (see table 3).

3.1 Ghost-gluon vertex on the lattice

On the lattice, the definition of the vertex renormalization function is obtained as was done in the continuum (see section 2). The only difference is that, from the weak-coupling expansion (or “perturbative” expansion) on the lattice, one obtains that the ghost-gluon vertex is given at tree level by [54]

$$\Gamma_{\mu}^{abc}(\tilde{k}, \tilde{q}) = i g_0 f^{abc} \hat{q}_{\mu} \cos\left(\frac{\pi \tilde{s}_{\mu} a}{L_{\mu}}\right), \quad (3.14)$$

where $\tilde{s} = \tilde{k} + \tilde{q}$. Clearly, by taking the formal continuum limit $a \rightarrow 0$ of the quantity $\Gamma_{\mu}^{abc}(\tilde{k}, \tilde{q})/a$ one recovers the continuum tree-level result (2.6). Then, in the case $\tilde{k} = 0$, $\tilde{s} = \tilde{q}$, equation (2.15) is still valid on the lattice if one sets

$$\Xi(\tilde{q}) = \frac{-i}{\hat{q}^2} \sum_{\mu} \frac{\hat{q}_{\mu}}{\cos\left(\frac{\pi \tilde{q}_{\mu} a}{L_{\mu}}\right)} \Gamma_{\mu}(0, \tilde{q}) \quad (3.15)$$

with

$$\Gamma_\mu(0, \tilde{q}) = \frac{1}{g_0 N_c (N_c^2 - 1)} \sum_{a,b,c} f^{abc} \Gamma_\mu^{abc}(0, \tilde{q}) \quad (3.16)$$

$$\Gamma_\mu^{abc}(0, \tilde{q}) = \frac{G_\mu^{abc}(0, \tilde{q})}{D(0) G^2(\tilde{q})} \quad (3.17)$$

and

$$\hat{q} = \left(\sum_{\mu=1}^4 \hat{q}_\mu^2 \right)^{1/2}, \quad (3.18)$$

where \hat{q}_μ is defined in terms of \tilde{q}_μ in equation (3.5). Thus, as in the continuum, we can write

$$\Xi(\tilde{q}) = \frac{1}{g_0 N_c (N_c^2 - 1)} \frac{1}{\hat{q}^2} \sum_\mu \frac{\hat{q}_\mu}{\cos\left(\frac{\pi \tilde{q}_\mu a}{L_\mu}\right)} \sum_{a,b,c} f^{abc} \text{Im} \Gamma_\mu^{abc}(0, \tilde{q}). \quad (3.19)$$

In order to check for possible effects due to the breaking of rotational symmetry, in our simulations we use two types of lattice momenta, i.e. $\tilde{q}_1 = \tilde{q}_2 = \tilde{q}_3 = 0, \tilde{q}_4 = \tilde{q}$ and $\tilde{q}_1 = \tilde{q}_2 = \tilde{q}_3 = \tilde{q}_4 = \tilde{q}$. In the following we will indicate the first type of momenta as *asymmetric* and the second one as *symmetric*. Clearly, using the relations $L_1 = L_2 = L_3 = L_4 = L$, we have

$$\hat{q} = \hat{q}_4 = 2 \sin\left(\frac{\pi \tilde{q} a}{L}\right) \quad (3.20)$$

in the asymmetric case and

$$\hat{q}_\mu = 2 \sin\left(\frac{\pi \tilde{q} a}{L}\right) \quad (3.21)$$

$$\hat{q} = 4 \sin\left(\frac{\pi \tilde{q} a}{L}\right) \quad (3.22)$$

in the symmetric one. Then, the quantity $\Xi(\tilde{q})$ above becomes

$$\Xi(\tilde{q}) = \frac{1}{g_0 N_c (N_c^2 - 1)} \frac{1}{\hat{q}} \frac{1}{\cos\left(\frac{\pi \tilde{q} a}{L}\right)} \sum_{a,b,c} f^{abc} \text{Im} \Gamma_4^{abc}(0, \tilde{q}) \quad (3.23)$$

in the asymmetric case and

$$\Xi(\tilde{q}) = \frac{1}{g_0 N_c (N_c^2 - 1)} \frac{1}{\hat{q}} \frac{1}{2 \cos\left(\frac{\pi \tilde{q} a}{L}\right)} \sum_\mu \sum_{a,b,c} f^{abc} \text{Im} \Gamma_\mu^{abc}(0, \tilde{q}) \quad (3.24)$$

in the symmetric one. Using the trigonometric relation $\sin(2\theta) = 2 \sin(\theta) \cos(\theta)$ these formulae can be rewritten as

$$\Xi(\tilde{q}) = \frac{1}{\sin\left(\frac{2\pi \tilde{q} a}{L}\right)} \Sigma(\tilde{q}), \quad (3.25)$$

where

$$\Sigma(\tilde{q}) = \frac{1}{g_0 N_c (N_c^2 - 1)} \sum_{a,b,c} f^{abc} \text{Im} \Gamma_4^{abc}(0, \tilde{q}) \quad (3.26)$$

in the asymmetric case and

$$\Sigma(\tilde{q}) = \frac{1}{g_0 N_c (N_c^2 - 1)} \sum_{a,b,c} f^{abc} \text{Im} \frac{1}{4} \sum_{\mu} \Gamma_{\mu}^{abc}(0, \tilde{q}) \quad (3.27)$$

in the symmetric one.

Finally, using equations (2.3), (2.4) and (3.11) we obtain

$$G_{\mu}^{abc}(0, \tilde{q}) = V \left\langle A_{\mu}^a(0) (M^{-1})^{bc}(\tilde{q}) \right\rangle, \quad (3.28)$$

where

$$A_{\mu}^a(0) = \frac{1}{V} \sum_x A_{\mu}^a(x) \quad (3.29)$$

and V is the lattice volume. Then, we can write

$$\Gamma_{\mu}^{abc}(0, \tilde{q}) = \frac{V \left\langle A_{\mu}^a(0) (M^{-1})^{bc}(\tilde{q}) \right\rangle}{D(0) G^2(\tilde{q})}. \quad (3.30)$$

With our notation, in the naive continuum limit $a \rightarrow 0$, the lattice quantity $4 a^2 D(\tilde{q})/g_0^2$ (respectively $a^2 G(\tilde{q})$) approaches the (continuum) propagator $D(q^2)$ (respectively $G(q^2)$). At the same time, we have that $2 A_{\mu}^a(0)/(a g_0) \rightarrow A_{\mu}^a(0)$ and $a^2 (M^{-1})^{bc}(\tilde{q}) \rightarrow (M^{-1})^{bc}(q)$. This implies that the (normalized) lattice ghost-gluon vertex $g_0 \Gamma_{\mu}^{abc}(0, \tilde{q})/(2a)$ approaches the quantity $\Gamma_{\mu}^{abc}(0, q)$ in the continuum limit. Also, since $\hat{q} \rightarrow a q$ when $a \rightarrow 0$, it is easy to verify that $\tilde{Z}_1^{-1}(\tilde{q}) = \Xi(\tilde{q})$ is dimensionless.

As said in the Introduction, in reference [29] the ghost-gluon renormalization function $\tilde{Z}_1(p^2)$ was indirectly evaluated. To this end the authors considered equation (1.1), which can be written as

$$Z_3(p^2, \beta) \tilde{Z}_3^2(p^2, \beta) = \frac{\alpha_s(p^2)}{\alpha_0(\beta)} \tilde{Z}_1^2(p^2, \beta), \quad (3.31)$$

where the β dependence is now indicated explicitly. The renormalization functions $Z_3(p^2, \beta)$ and $\tilde{Z}_3^2(p^2, \beta)$ can be evaluated using the matching technique described in detail in [55, section III]. Then, one can show [29] that the left-hand side of the above equation rises linearly with $-\ln(\sigma a^2)$, where σ is the string tension. At the same time, for large enough β values one finds that [29]

$$\frac{1}{\alpha_0(\beta)} \propto -\ln(\sigma a^2) + \text{constant}, \quad (3.32)$$

where the constant is β -independent. It follows that $\tilde{Z}_1^2(p^2, \beta)$ must be finite in the continuum limit, if the renormalized coupling $\alpha_s(p^2)$ is assumed finite. Of course, this approach does not allow either an effective determination of the vertex renormalization function or a study of its p dependence. These are the main goals of the present work.

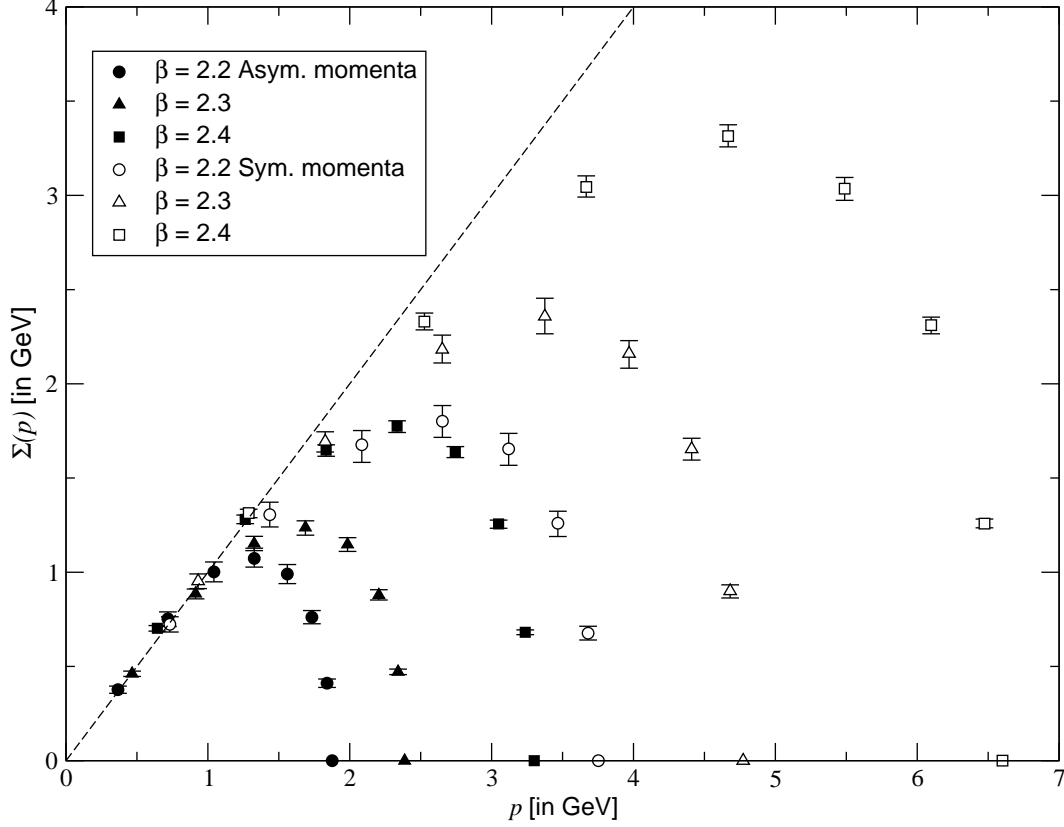


Figure 4: Results for $\Sigma(p)$ for the lattice volume $V = 16^4$ as a function of $p = \hat{p}/a$ in GeV, considering asymmetric and symmetric momenta. Error bars were obtained using the bootstrap method with 250 samples. The dashed line represents the tree-level momentum dependence ($\sim p$) of the vertex function in the continuum.

4. Results

We have evaluated the reduced ghost-gluon vertex function $\Gamma_\mu^{abc}(0, \tilde{p})$ at the asymmetric point $(0; \tilde{p}, -\tilde{p})$ using equation (3.30), in the SU(2) case. (Let us recall that when $N_c = 2$ the structure functions f^{abc} are given by the completely anti-symmetric tensor ϵ^{abc} .) Results for the quantity $\Sigma(\tilde{p})$, defined in equations (3.26) and (3.27), and for $\tilde{Z}_1^{-1}(\tilde{p}) = \Xi(\tilde{p})$ (see equation (3.25)) as a function of $p = \hat{p}/a$ (in physical units) are reported in figures 4 and 5. We consider for these figures the lattice volume $V = 16^4$, for both asymmetric and symmetric momenta. Error bars were obtained using the bootstrap method with 250 samples. (We checked that the results do not change when considering 500 samples.) We find that the function $\Sigma(\tilde{p})$ has the same momentum dependence as the tree-level vertex (i.e. $\sim \hat{p} \cos(\pi \tilde{p} a/L) \sim \sin(2\pi \tilde{p} a/L)$) and that (consequently) $\tilde{Z}_1(\tilde{p})$ is approximately constant and equal to 1.

As explained in section 3 above, in order to check for Gribov-copy effects we have considered two different gauge fixing methods for each thermalized configuration, the second of which employs the so-called smeared gauge fixing. Let us recall that Gribov-copy effects have been found for the ghost propagator in Landau gauge, at least in the small-momentum

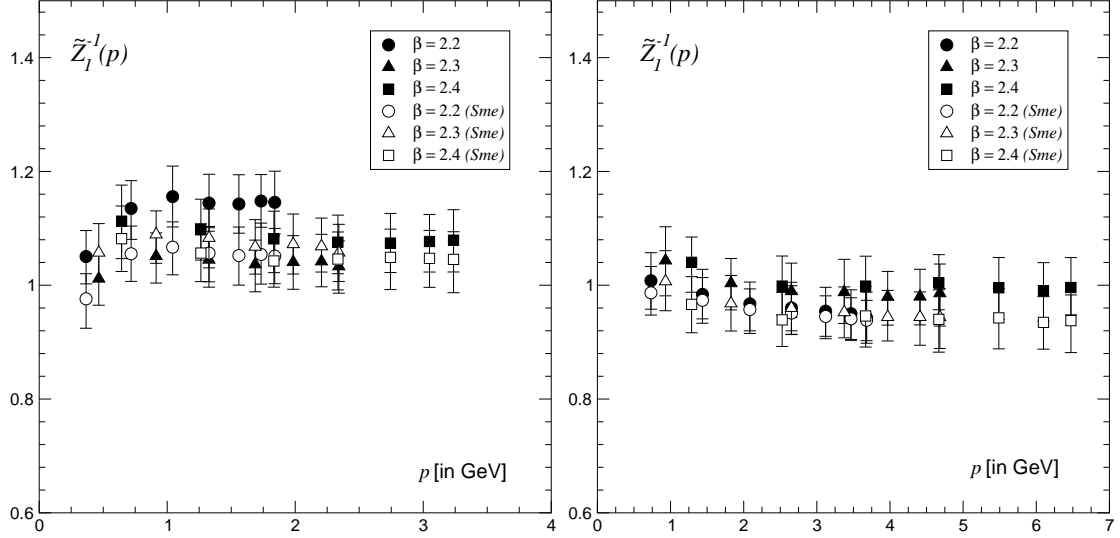


Figure 5: Results for $\tilde{Z}_1^{-1}(p)$ for the lattice volume $V = 16^4$ as a function of $p = \hat{p}/a$ in GeV, considering asymmetric (left) and symmetric (right) momenta. In both cases we show data obtained considering the two different gauge-fixing methods (without and with smearing). Error bars were obtained using the bootstrap method with 250 samples.

limit [36, 52, 53, 56]. Recently, such effects were also found for the gluon propagator in the infrared region [57]. In figure 5 are also shown the data for $\tilde{Z}_1^{-1}(\tilde{p})$ obtained for the lattice volume $V = 16^4$ using the smeared gauge-fixing. The $\tilde{Z}_1^{-1}(\tilde{p})$ data for all lattice volumes and β values considered in this work are reported in tables 4 (asymmetric momenta) and 5 (symmetric momenta) considering the two different gauge-fixing methods (without and with smearing). We can clearly see that $\tilde{Z}_1^{-1}(\tilde{p})$ decreases as the lattice volume increases for a fixed coupling β and that for $V = 16^4$ the dependence of $\tilde{Z}_1^{-1}(\tilde{p})$ on the coupling β , on the type of momenta and on Gribov-copy effects is relatively small. This is also evident if we try to fit the data for $\tilde{Z}_1^{-1}(\tilde{p})$ to a constant (see table 6). Nevertheless, it is clear that data obtained using the smeared gauge-fixing are generally smaller than those obtained without smearing.

It is difficult to explain the small variations in the results for $\tilde{Z}_1^{-1}(\tilde{p})$ when considering asymmetric and symmetric momenta or the smeared gauge fixing compared to the standard gauge fixing. Indeed, several quantities enter the definition of $\Gamma_\mu^{abc}(0, \tilde{p})$ [see equation (3.30)] and therefore the evaluation of $\tilde{Z}_1^{-1}(\tilde{p})$. A more detailed study (see tables 7, 8 and 9) of the gluon propagator at zero momentum $D(0)$, the ghost propagator $G(\tilde{p})$ for $\tilde{p}_1 = \tilde{p}_2 = \tilde{p}_3 = 0, \tilde{p}_4 = N/2$ and the quantity $\sum_{a,b,c} f^{abc} \text{Im} \langle A_\mu^a(0) (M^{-1})^{bc}(\tilde{p}) \rangle$ as a function of $p = \hat{p}/a$ does not clarify the situation. In particular, the Gribov-copy effects, if present, are always small and within error bars. This is not surprising, since we are considering relatively small lattice volumes in the scaling region. We can conclude that the small systematic variations in the results of $\tilde{Z}_1(\tilde{p})$ are probably related to correlations among data at different momenta, since they have been obtained using the same set of configurations.

Finally, we can use our data to evaluate the running coupling constant $\alpha_s(p^2)$ using equation (1.1). For $\tilde{Z}_1(p^2)$ we take the fit to a constant reported in table 6. The results

p (GeV)	0.366	0.718	1.04	1.33	1.56	1.73	1.84
$N = 4$	-	-	-	1.40(5)	-	-	-
$N = 4$, sme	-	-	-	1.39(4)	-	-	-
$N = 8$	-	1.08(5)	-	1.11(4)	-	1.13(5)	-
$N = 8$, sme	-	1.10(5)	-	1.12(4)	-	1.14(4)	-
$N = 16$	1.05(5)	1.13(5)	1.16(5)	1.14(5)	1.14(5)	1.15(5)	1.15(5)
$N = 16$, sme	0.98(5)	1.06(5)	1.07(5)	1.06(5)	1.05(5)	1.05(5)	1.05(5)
p (GeV)	0.466	0.913	1.33	1.69	1.98	2.20	2.34
$N = 4$	-	-	-	1.31(4)	-	-	-
$N = 4$, sme	-	-	-	1.30(4)	-	-	-
$N = 8$	-	1.30(5)	-	1.22(5)	-	1.21(5)	-
$N = 8$, sme	-	1.24(6)	-	1.18(5)	-	1.18(5)	-
$N = 16$	1.01(4)	1.05(4)	1.05(5)	1.04(5)	1.04(5)	1.04(5)	1.03(4)
$N = 16$, sme	1.06(5)	1.09(5)	1.08(5)	1.07(5)	1.07(5)	1.07(5)	1.06(5)
p (GeV)	0.644	1.26	1.83	2.34	2.75	3.05	3.24
$N = 4$	-	-	-	1.36(4)	-	-	-
$N = 4$, sme	-	-	-	1.35(3)	-	-	-
$N = 8$	-	1.16(5)	-	1.06(5)	-	1.06(4)	-
$N = 8$, sme	-	1.15(5)	-	1.07(5)	-	1.06(4)	-
$L = 16$	1.11(6)	1.10(5)	1.08(5)	1.08(5)	1.07(5)	1.08(5)	1.08(5)
$N = 16$, sme	1.08(6)	1.06(5)	1.04(5)	1.05(5)	1.05(5)	1.05(5)	1.05(5)

Table 4: Results for $\tilde{Z}_1^{-1}(\tilde{p})$ as a function of $p = \hat{p}/a$ (in GeV) for the three lattice sides $N = 4, 8, 16$ and the three β values considered (i.e. 2.2, 2.3 and 2.4, respectively top, center and bottom part of the table) in the case of asymmetric momenta, considering the two different gauge-fixing methods (without and with smearing). Error bars were obtained using the bootstrap method with 250 samples.

are shown in figure 6. We can see that data obtained at different β values do not lie on a single curve. This is probably related to the fact that our data are not at infinite volume. Indeed, this is a well-known effect for the gluon field when evaluated at zero momentum [59, 58, 60, 61, 62].

5. Conclusions

We have presented the first numerical study of the reduced ghost-gluon vertex function $\Gamma_\mu^{abc}(0, p)$ and of the renormalization function $\tilde{Z}_1(p^2)$ in minimal Landau gauge. We have considered the SU(2) case and the asymmetric point $(0; p, -p)$. We found that the vertex function has the same momentum dependence of the tree-level vertex and that $\tilde{Z}_1(p^2)$ is approximately constant and equal to 1, at least for momenta $p \gtrsim 1$ GeV. This is a direct nonperturbative verification of the well-known perturbative result that $\tilde{Z}_1(p^2)$ is finite and constant to all orders of perturbation theory [2, 3]. In particular, using the result obtained at the largest value of β considered here (i.e. $\beta = 2.4$) we can write $\tilde{Z}_1^{-1}(p^2) = 1.02_{-7}^{+6}$ (see table 6), where errors include Gribov-copy effects and discretization errors related to the breaking of rotational invariance.

p (GeV)	0.732	1.44	2.08	2.65	3.12	3.47	3.68
$N = 4$	-	-	-	1.22(4)	-	-	-
$N = 4, \text{ sme}$	-	-	-	1.23(4)	-	-	-
$N = 8$	-	1.07(5)	-	1.01(5)	-	0.99(5)	-
$N = 8, \text{ sme}$	-	1.03(5)	-	0.98(5)	-	0.97(5)	-
$N = 16$	1.01(5)	0.98(4)	0.97(4)	0.96(4)	0.95(4)	0.95(4)	0.94(5)
$N = 16, \text{ sme}$	0.99(4)	0.97(4)	0.96(4)	0.95(4)	0.95(4)	0.94(4)	0.94(5)
p (GeV)	0.931	1.83	2.65	3.37	3.97	4.41	4.68
$N = 4$	-	-	-	1.14(4)	-	-	-
$N = 4, \text{ sme}$	-	-	-	1.12(4)	-	-	-
$N = 8$	-	1.13(6)	-	1.05(5)	-	1.03(5)	-
$N = 8, \text{ sme}$	-	1.03(5)	-	0.97(5)	-	0.95(5)	-
$N = 16$	1.04(6)	1.00(4)	0.99(5)	0.99(6)	0.98(5)	0.98(5)	0.99(5)
$N = 16, \text{ sme}$	1.01(5)	0.97(5)	0.96(5)	0.95(4)	0.94(4)	0.94(5)	0.94(5)
p (GeV)	1.29	2.53	3.67	4.67	5.49	6.10	6.48
$N = 4$	-	-	-	1.21(4)	-	-	-
$N = 4, \text{ sme}$	-	-	-	1.16(4)	-	-	-
$N = 8$	-	1.17(7)	-	1.05(5)	-	1.03(5)	-
$N = 8, \text{ sme}$	-	1.17(7)	-	1.04(4)	-	1.02(5)	-
$N = 16$	1.04(5)	1.00(5)	1.00(5)	1.00(5)	1.00(5)	0.99(5)	1.00(5)
$N = 16, \text{ sme}$	0.97(5)	0.94(5)	0.95(5)	0.94(6)	0.94(5)	0.94(5)	0.94(5)

Table 5: Results for $\tilde{Z}_1^{-1}(\tilde{p})$ as a function of $p = \hat{p}/a$ (in GeV) for the three lattice sides $N = 4, 8, 16$ and the three β values considered (i.e. 2.2, 2.3 and 2.4, respectively top, center and bottom part of the table) in the case of symmetric momenta, considering the two different gauge-fixing methods (without and with smearing). Error bars were obtained using the bootstrap method with 250 samples.

	asymmetric momenta	symmetric momenta
$\beta = 2.2$	1.148(4)	0.960(6)
$\beta = 2.2, \text{ sme}$	1.056(4)	0.952(5)
$\beta = 2.3$	1.039(3)	0.989(3)
$\beta = 2.3, \text{ sme}$	1.070(3)	0.949(5)
$\beta = 2.4$	1.082(4)	1.004(6)
$\beta = 2.4, \text{ sme}$	1.050(3)	0.946(4)

Table 6: Constant fits of the $\tilde{Z}_1^{-1}(\tilde{p})$ data reported in tables 4 and 5 for the lattice volume $V = 16^4$ considering momenta $p \geq 1$ GeV.

We are now extending this study, considering larger lattice volumes (and therefore smaller momenta), the symmetric point $k^2 = q^2 = s^2$, the $3d$ case and the $SU(3)$ gauge group. A significant improvement of our results for $\alpha_s(p^2)$ may be expected by considering the symmetric point.

	$V = 4^4$	$V = 8^4$	$V = 16^4$
$\beta = 2.2$	5.33(6)	11.6(3)	14.5(4)
$\beta = 2.2, \text{ sme}$	5.38(6)	11.8(2)	14.4(3)
$\beta = 2.3$	6.17(7)	18.9(4)	31.7(7)
$\beta = 2.3, \text{ sme}$	6.23(7)	19.3(4)	32.4(7)
$\beta = 2.4$	6.87(8)	23.5(5)	53(1)
$\beta = 2.4, \text{ sme}$	6.94(8)	23.8(5)	53(1)

Table 7: Results for the gluon propagator at zero momentum $D(0)$ (in lattice units) for the three lattice sides ($N = 4, 8, 16$) and the three β values (i.e. 2.2, 2.3 and 2.4) considering the two different gauge-fixing methods (without and with smearing). Error bars were obtained using the bootstrap method with 250 samples.

	$V = 4^4$	$V = 8^4$	$V = 16^4$
$\beta = 2.2$	0.353(1)	0.3174(5)	0.3098(3)
$\beta = 2.2, \text{ sme}$	0.352(1)	0.3175(5)	0.3097(3)
$\beta = 2.3$	0.340(1)	0.3075(4)	0.2998(2)
$\beta = 2.3, \text{ sme}$	0.340(1)	0.3075(4)	0.2997(2)
$\beta = 2.4$	0.334(1)	0.3013(4)	0.2946(3)
$\beta = 2.4, \text{ sme}$	0.333(1)	0.3013(4)	0.2945(3)

Table 8: Results for the ghost propagator $G(p)$ (in lattice units), evaluated at the asymmetric momentum with components $\tilde{p}_1 = \tilde{p}_2 = \tilde{p}_3 = 0$ and $\tilde{p}_4 = N/2$, for the three lattice sides ($N = 4, 8, 16$) and the three β values (i.e. 2.2, 2.3 and 2.4) considering the two different gauge-fixing methods (without and with smearing). Error bars were obtained using the bootstrap method with 250 samples.

Acknowledgments

This work was supported by Fundação de Amparo à Pesquisa do Estado de São Paulo (FAPESP) through grants: 00/05047–5 (AC, TM) and 03/00928–1 (AM). Partial support from Conselho Nacional de Desenvolvimento Científico e Tecnológico (CNPq) is also acknowledged (AC, TM).

References

- [1] T. Muta, *Foundations of quantum chromodynamics*, World Scientific, Singapore 1987.
- [2] J.C. Taylor, *Ward identities and charge renormalization of the Yang-Mills field*, *Nucl. Phys.* **B 33** (1971) 436.
- [3] O. Piguet and S.P. Sorella, *Algebraic renormalization: perturbative renormalization, symmetries and anomalies*, *Lect. Notes Phys.* **M28** (1995) 1.
- [4] L. von Smekal, R. Alkofer and A. Hauck, *The infrared behavior of gluon and ghost propagators in Landau gauge QCD*, *Phys. Rev. Lett.* **79** (1997) 3591 [[hep-ph/9705242](#)].
- [5] L. von Smekal, A. Hauck and R. Alkofer, *A solution to coupled Dyson-Schwinger equations for gluons and ghosts in Landau gauge*, *Ann. Phys. (NY)* **267** (1998) 1 [[hep-ph/9707327](#)].

p (GeV)	0.366	0.718	1.04	1.33	1.56	1.73	1.84
$N = 16$	0.28(2)	0.019(1)	0.0041(2)	0.00143(7)	0.00062(3)	0.00029(2)	0.000122(6)
$N = 16, \text{ sme}$	0.26(2)	0.0177(9)	0.0038(2)	0.00131(7)	0.00057(3)	0.00027(1)	0.000111(6)
p (GeV)	0.466	0.913	1.33	1.69	1.98	2.20	2.34
$N = 16$	0.46(3)	0.031(2)	0.0069(4)	0.0025(1)	0.00113(6)	0.00054(3)	0.00023(1)
$N = 16, \text{ sme}$	0.48(4)	0.032(2)	0.0073(4)	0.0026(1)	0.00118(7)	0.00057(3)	0.00024(1)
p (GeV)	0.644	1.26	1.83	2.34	2.75	3.05	3.24
$N = 16$	0.74(7)	0.046(3)	0.0108(6)	0.0040(2)	0.0018(1)	0.00089(5)	0.00037(2)
$N = 16, \text{ sme}$	0.70(6)	0.045(3)	0.0106(6)	0.0039(2)	0.0018(1)	0.00087(5)	0.00037(2)

Table 9: Results for the quantity $\sum_{a,b,c} f^{abc} \text{Im} \langle A_\mu^a(0) (M^{-1})^{bc}(\tilde{p}) \rangle$ as a function of $p = \hat{p}/a$ (in GeV) for the lattice side $N = 16$ and the three β values considered (i.e. 2.2, 2.3 and 2.4, respectively top, center and bottom part of the table) in the case of asymmetric momenta, considering the two different gauge-fixing methods (without and with smearing). Error bars were obtained using the bootstrap method with 250 samples.

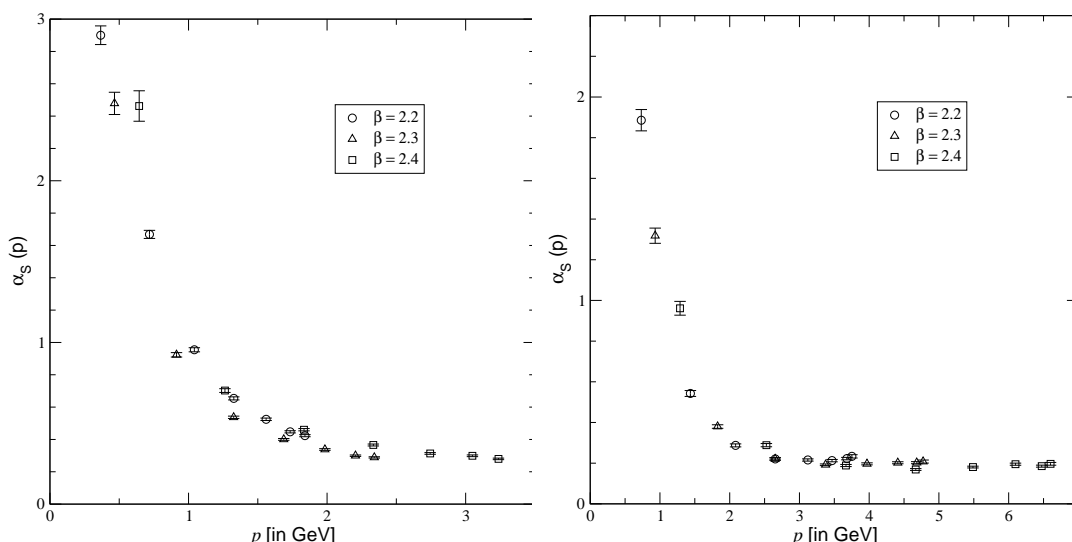


Figure 6: Results for the running coupling $\alpha_s(p)$ as a function $p = \hat{p}/a$ in GeV, considering asymmetric (left) and symmetric (right) momenta. Here we use the standard gauge-fixing method (without smearing). Error bars were obtained using the bootstrap method with 250 samples.

- [6] R. Alkofer and L. von Smekal, *The infrared behavior of QCD Green's functions: Confinement, dynamical symmetry breaking, and hadrons as relativistic bound states*, *Phys. Rept.* **353** (2001) 281 [[hep-ph/0007355](#)].
- [7] D. Atkinson and J.C.R. Bloch, *Running coupling in non-perturbative QCD, 1. Bare vertices and y-max approximation*, *Phys. Rev.* **D 58** (1998) 094036 [[hep-ph/9712459](#)].
- [8] D. Atkinson and J.C.R. Bloch, *QCD in the infrared with exact angular integrations*, *Mod. Phys. Lett.* **A 13** (1998) 1055 [[hep-ph/9802239](#)].
- [9] J.C.R. Bloch, *Multiplicative renormalizability of gluon and ghost propagators in QCD*, *Phys. Rev.* **D 64** (2001) 116011 [[hep-ph/0106031](#)].

- [10] D. Zwanziger, *Non-perturbative Landau gauge and infrared critical exponents in QCD*, *Phys. Rev. D* **65** (2002) 094039 [[hep-th/0109224](#)].
- [11] C. Lerche and L. von Smekal, *On the infrared exponent for gluon and ghost propagation in Landau gauge QCD*, *Phys. Rev. D* **65** (2002) 125006 [[hep-ph/0202194](#)].
- [12] C.S. Fischer and R. Alkofer, *Infrared exponents and running coupling of SU(N) Yang-Mills theories*, *Phys. Lett. B* **536** (2002) 177 [[hep-ph/0202202](#)].
- [13] C.S. Fischer, R. Alkofer and H. Reinhardt, *The elusiveness of infrared critical exponents in Landau gauge Yang-Mills theories*, *Phys. Rev. D* **65** (2002) 094008 [[hep-ph/0202195](#)].
- [14] R. Alkofer, W. Detmold, C.S. Fischer and P. Maris, *Analytic properties of the Landau gauge gluon and quark propagators*, *Phys. Rev. D* **70** (2004) 014014 [[hep-ph/0309077](#)].
- [15] R. Alkofer, W. Detmold, C.S. Fischer and P. Maris, *Analytic structure of the gluon and quark propagators in Landau gauge QCD*, [hep-ph/0309078](#).
- [16] D. Zwanziger, *Time-independent stochastic quantization, Dyson-Schwinger equations, and infrared critical exponents in QCD*, *Phys. Rev. D* **67** (2003) 105001 [[hep-th/0206053](#)].
- [17] J.C.R. Bloch, *Two loop improved truncation of the ghost-gluon Dyson-Schwinger equations: multiplicatively renormalizable propagators and nonperturbative running coupling*, *Few Body Syst.* **33** (2003) 111 [[hep-th/0303125](#)].
- [18] J.M. Pawłowski, D.F. Litim, S. Nedelko and L. von Smekal, *Infrared behaviour and fixed points in Landau gauge QCD*, *Phys. Rev. Lett.* **93** (2004) 152002 [[hep-th/0312324](#)].
- [19] K.-I. Kondo, *Implications of analyticity to mass gap, color confinement and infrared fixed point in Yang-Mills theory*, [hep-th/0303251](#).
- [20] K.-I. Kondo, *Gluon and ghost propagators from the viewpoint of general principles of quantized gauge field theories*, *Nucl. Phys.* **129** (Proc. Suppl.) (2004) 715 [[hep-lat/0309142](#)].
- [21] R.F. Sobreiro, S.P. Sorella, D. Dudal and H. Verschelde, *Gribov horizon in the presence of dynamical mass generation in euclidean Yang-Mills theories in the Landau gauge*, *Phys. Lett. B* **590** (2004) 265 [[hep-th/0403135](#)].
- [22] R.F. Sobreiro, S.P. Sorella, D. Dudal and H. Verschelde, *Remarks on the gribov horizon and dynamical mass generation in euclidean Yang-Mills theories*, [hep-th/0406161](#).
- [23] A.C. Aguilar, Ph.D. thesis, IFT–Universidade Estadual Paulista, March 2004 (in Portuguese).
- [24] A.C. Aguilar and A.A. Natale, *A dynamical gluon mass solution in Mandelstam’s approximation*, [hep-ph/0405024](#).
- [25] C.S. Fischer and H. Gies, *Renormalization flow of Yang-Mills propagators*, *J. High Energy Phys.* **10** (2004) 048 [[hep-ph/0408089](#)].
- [26] A. Cucchieri, T. Mendes and D. Zwanziger, *SU(2) running coupling constant and confinement in minimal Coulomb and Landau gauges*, *Nucl. Phys.* **106** (Proc. Suppl.) (2002) 697 [[hep-lat/0110188](#)].
- [27] J.C.R. Bloch, A. Cucchieri, K. Langfeld and T. Mendes, *Running coupling constant and propagators in SU(2) Landau gauge*, *Nucl. Phys.* **119** (Proc. Suppl.) (2003) 736 [[hep-lat/0209040](#)].
- [28] K. Langfeld et al., *Vortex induced confinement and the IR properties of Green functions*, [hep-th/0209173](#).

- [29] J.C.R. Bloch, A. Cucchieri, K. Langfeld and T. Mendes, *Propagators and running coupling from SU(2) lattice gauge theory*, *Nucl. Phys. B* **687** (2004) 76 [[hep-lat/0312036](#)].
- [30] UKQCD collaboration, D.B. Leinweber, J.I. Skullerud, A.G. Williams and C. Parrinello, *Asymptotic scaling and infrared behavior of the gluon propagator*, *Phys. Rev. D* **60** (1999) 094507 [[hep-lat/9811027](#)].
- [31] F.D.R. Bonnet, P.O. Bowman, D.B. Leinweber, A.G. Williams and J.M. Zanotti, *Infinite volume and continuum limits of the Landau-gauge gluon propagator*, *Phys. Rev. D* **64** (2001) 034501 [[hep-lat/0101013](#)].
- [32] H. Nakajima and S. Furui, *Numerical studies of confinement in the Landau gauge by the larger lattice simulation*, *Nucl. Phys. B* **119** (Proc. Suppl.) (2003) 730 [[hep-lat/0208074](#)].
- [33] H. Nakajima and S. Furui, *Color confinement in lattice Landau gauge*, [hep-lat/0303024](#).
- [34] S. Furui and H. Nakajima, *Infrared features of lattice Landau gauge QCD and the Gribov copy problem*, *AIP Conf. Proc.* **717** (2004) 685 [[hep-lat/0309166](#)].
- [35] S. Furui and H. Nakajima, *Infrared features of the Landau gauge QCD*, *Phys. Rev. D* **69** (2004) 074505 [[hep-lat/0305010](#)].
- [36] H. Nakajima and S. Furui, *Infrared features of the lattice Landau gauge QCD*, *Nucl. Phys. B* **129** (Proc. Suppl.) (2004) 730 [[hep-lat/0309165](#)].
- [37] S. Furui and H. Nakajima, *What the Gribov copy tells on the confinement and the theory of dynamical chiral symmetry breaking*, [hep-lat/0403021](#).
- [38] S. Furui and H. Nakajima, *Colour confinement in the lattice Landau gauge QCD simulation*, [hep-lat/0012017](#).
- [39] A. Mihara, A. Cucchieri and T. Mendes, *Numerical study of the ghost-ghost-gluon vertex on the lattice*, [hep-lat/0408021](#).
- [40] A. Cucchieri, T. Mendes, G. Travieso and A.R. Taurines, *Parallel implementation of a lattice-gauge-theory code: studying quark confinement on pc clusters*, [hep-lat/0308005](#).
- [41] M. Creutz, *Monte Carlo study of quantized SU(2) gauge theory*, *Phys. Rev. D* **21** (1980) 2308.
- [42] S.L. Adler, *Algorithms for pure gauge theory*, *Nucl. Phys. B* **9** (Proc. Suppl.) (1989) 437.
- [43] F.R. Brown and T.J. Woch, *Overrelaxed heat bath and metropolis algorithms for accelerating pure gauge Monte Carlo calculations*, *Phys. Rev. Lett.* **58** (1987) 2394.
- [44] U. Wolff, *Dynamics of hybrid overrelaxation in the gaussian model*, *Phys. Lett. B* **288** (1992) 166.
- [45] A. Cucchieri and T. Mendes, *Critical slowing-down in SU(2) Landau gauge-fixing algorithms*, *Nucl. Phys. B* **471** (1996) 263 [[hep-lat/9511020](#)].
- [46] A. Cucchieri and T. Mendes, *Study of critical slowing-down in SU(2) Landau gauge fixing*, *Nucl. Phys. B* **53** (Proc. Suppl.) (1997) 811 [[hep-lat/9608051](#)].
- [47] A. Cucchieri and T. Mendes, *Critical slowing-down in SU(2) Landau-gauge-fixing algorithms at $\beta = \infty$* , *Comput. Phys. Commun.* **154** (2003) 1 [[hep-lat/0301019](#)].
- [48] D. Zwanziger, *Fundamental modular region, Boltzmann factor and area law in lattice gauge theory*, *Nucl. Phys. B* **412** (1994) 657.

- [49] A. Cucchieri, *Numerical study of the fundamental modular region in the minimal Landau gauge*, *Nucl. Phys. B* **521** (1998) 365 [[hep-lat/9711024](#)].
- [50] J.E. Hetrick and P. de Forcrand, *Smeared gauge fixing*, *Nucl. Phys.* **63** (Proc. Suppl.) (1998) 838 [[hep-lat/9710003](#)].
- [51] P. Marenzoni and P. Rossi, *Gribov copies in lattice QCD*, *Phys. Lett. B* **311** (1993) 219 [[hep-lat/9306010](#)].
- [52] A. Cucchieri, *Gribov copies in the minimal Landau gauge: the influence on gluon and ghost propagators*, *Nucl. Phys. B* **508** (1997) 353 [[hep-lat/9705005](#)].
- [53] A. Cucchieri and T. Mendes, *I: the influence of Gribov copies on gluon and ghost propagators in Landau gauge. II: a new implementation of the Fourier acceleration method*, *Nucl. Phys.* **63** (Proc. Suppl.) (1998) 841 [[hep-lat/9710040](#)].
- [54] H. Kawai, R. Nakayama and K. Seo, *Comparison of the lattice Λ parameter with the continuum Λ parameter in massless QCD*, *Nucl. Phys. B* **189** (1981) 40.
- [55] A. Cucchieri, T. Mendes and A.R. Taurines, *SU(2) Landau gluon propagator on a 140^3 lattice*, *Phys. Rev. D* **67** (2003) 091502 [[hep-lat/0302022](#)].
- [56] T.D. Bakeev, E.-M. Ilgenfritz, V.K. Mitrjushkin and M. Mueller-Preussker, *On practical problems to compute the ghost propagator in SU(2) lattice gauge theory*, *Phys. Rev. D* **69** (2004) 074507 [[hep-lat/0311041](#)].
- [57] P.J. Silva and O. Oliveira, *Gribov copies, lattice QCD and the gluon propagator*, *Nucl. Phys. B* **690** (2004) 177 [[hep-lat/0403026](#)].
- [58] A. Cucchieri, *Infrared behavior of the gluon propagator in lattice Landau gauge: the three-dimensional case*, *Phys. Rev. D* **60** (1999) 034508 [[hep-lat/9902023](#)].
- [59] A. Cucchieri, *Infrared behavior of the gluon propagator in lattice Landau gauge*, *Phys. Lett. B* **422** (1998) 233 [[hep-lat/9709015](#)].
- [60] A. Cucchieri and D. Zwanziger, *Numerical study of gluon propagator and confinement scenario in minimal coulomb gauge*, *Phys. Rev. D* **65** (2002) 014001 [[hep-lat/0008026](#)].
- [61] A. Cucchieri and D. Zwanziger, *Fit to gluon propagator and Gribov formula*, *Phys. Lett. B* **524** (2002) 123 [[hep-lat/0012024](#)].
- [62] A. Cucchieri, F. Karsch and P. Petreczky, *Propagators and dimensional reduction of hot SU(2) gauge theory*, *Phys. Rev. D* **64** (2001) 036001 [[hep-lat/0103009](#)].